ELSEVIER

International Journal of Solids and Structures 40 (2003) 7329–7337

INTERNATIONAL JOURNAL OF SOLIDS and STRUCTURES

www.elsevier.com/locate/ijsolstr

Finite deformation continuum model for single-walled carbon nanotubes

X.-L. Gao *, K. Li

Department of Mechanical Engineering—Engineering Mechanics, Michigan Technological University, 1400 Townsend Drive, Houghton, MI 49931-1295, USA

Received 13 May 2003; received in revised form 4 September 2003

Abstract

A continuum-based model for computing strain energies and estimating Young's modulus of single-walled carbon nanotubes (SWCNTs) is developed by using an energy equivalence-based multi-scale approach. A SWCNT is viewed as a continuum hollow cylinder formed by rolling up a flat graphite sheet that is treated as an isotropic continuum plate. Kinematic analysis is performed on the continuum level, with the Hencky (true) strain and the Cauchy (true) stress being employed to account for finite deformations. Based on the equivalence of the strain energy and the molecular potential energy, a formula for calculating Young's modulus of SWCNTs is derived. This formula, containing both the molecular and continuum scale parameters, directly links macroscopic responses of nanotubes to their molecular structures. Sample numerical results show that the predictions by the new model compare favorably with those by several existing continuum and molecular dynamics models.

Keywords: Carbon nanotube; Continuum model; Young's modulus; Finite deformation; Strain energy; Molecular dynamics; Multi-scale modeling

1. Introduction

Carbon nanotubes have been found to exhibit extraordinary physical and mechanical properties (e.g., Thostenson et al., 2001; Maruyama and Alam, 2002; Bernholc et al., 2002; Qian et al., 2002). Consequently, they are identified as ideal reinforcing materials for high-performance nanocomposites (e.g., Vaia et al., 2001; Maruyama and Alam, 2002). To realize this goal, accurate understanding of the mechanical responses of individual carbon nanotubes and their behavior at the nanotube–matrix interface is essential.

A fairly large number of studies have been devoted to predicting elastic properties of carbon nanotubes by using empirical potential techniques, tight-binding methods and *ab initio* calculations. These approaches typically involve extensive computations and tend to be configuration specific. In contrast, analytical models based on continuum mechanics are known to be more cost-efficient and less geometry dependent.

* Corresponding author. Tel.: +1-906-487-1898; fax: +1-906-487-2822.
E-mail address: xgao@mtu.edu (X.-L. Gao).

0020-7683/$ - see front matter © 2003 Elsevier Ltd. All rights reserved.
doi:10.1016/j.ijsolstr.2003.09.009

However, extensive investigations on continuum models for nanotubes have not been undertaken until recently. By linking molecular structures of nanotubes to their macroscopic responses through energy equivalence, two continuum-based models for predicting elastic properties of nanotubes have recently been proposed by Odegard et al. (2002) and Li and Chou (2003). In another recent development by Zhang et al. (2002), a continuum theory for modeling carbon nanotubes is established by directly incorporating interatomic potentials into a continuum-level constitutive relation on the basis of the Cauchy–Born rule. These three continuum mechanics models are shown to give good predictions when compared with more detailed molecular dynamics models and existing experimental results, thereby supporting the development of continuum-based models using multi-scale approaches.

A single-walled carbon nanotube (SWCNT) can be viewed as a hollow cylinder formed by rolling up a two-dimensional (2-D) graphite sheet (e.g., Sawada and Hamada, 1992; Tersoff, 1992; Thostenson et al., 2001). Naturally, the formation of such a nanotube from a flat graphite sheet is a large deformation problem. Hence, kinematics of finite deformations should be employed in developing continuum-based models. However, existing continuum mechanics models for energetics of carbon nanotubes are built upon linear elasticity theories dealing with infinitesimal deformations. For example, the strain energy Π stored in a SWCNT of length L, thickness a and radius R (due to the afore-mentioned rolling up) has been taken to be of the form (e.g., Robertson et al., 1992; Gao et al., 1998):

$$\Pi = \frac{\pi E L a^3}{12R}, \tag{1}$$

where E is the Young's modulus. This formula was initially derived by Tibbetts (1984) for a different purpose using the Bernoulli–Euler (simple) beam bending theory based on infinitesimal displacement and plane stress assumptions. Therefore, L and a in Eq. (1) are actually properties of the flat (undeformed) graphite sheet from which the SWCNT is formed, and R is the radius of the neutral surface. In addition, it is required that L in Eq. (1), which is based on the simple beam bending theory for narrow (plane stress) beams, be small (compared with a) for accurate predictions. These facts set limitations for the use of Eq. (1) in calculating strain energies stored in nanotubes.

The objective of this paper is to develop a continuum-based model for computing strain energies and estimating Young's modulus of SWCNTs by using finite deformation kinematics and incorporating molecular structures. In Section 2, kinematic and constitutive relations, both on the continuum level, are first obtained. Hencky (true) strain and Cauchy (true) stress are used to account for large deformations, and Hooke's law is employed to describe the constitutive behavior. This is followed by the formulation of the boundary-value problem, which leads to explicit formulas for computing strain energies and effective Young's modulus of SWCNTs. The molecular structures of nanotubes are incorporated into the model through requiring the energy equivalence of the strain energy and the molecular potential energy. Numerical results of sample cases are presented in Section 3 to illustrate the application of the new formulas. A comparison with relevant data—modeling and experimental—is also given there. The paper concludes with a summary in Section 4.

2. Formulation

2.1. Kinematic and constitutive relations

The graphite sheet is represented as a 2-D continuum plate with a finite (effective) thickness before being rolled into a hollow cylinder equivalently representing the carbon nanotube mapped from the graphite sheet. This enables the kinematic analysis to be performed on the continuum level. By following a procedure similar to that used in Gao (1994), the kinematic relations can be derived as follows.

Let $\mathbf{X}$ and $\mathbf{r}$ be the position vectors of a material point in the undeformed and deformed configurations, respectively. Then, the mapping $\mathbf{X} \to \mathbf{r}$, i.e.,

$$\begin{aligned} &\mathbf{X} = X\mathbf{e_1} + Y\mathbf{e_2} + Z\mathbf{e_3}, \quad -T \leqslant X \leqslant T, \ -W \leqslant Y \leqslant W, \ -L \leqslant Z \leqslant L, \\ &\to \mathbf{r} = r\mathbf{e}_r(\theta) + z\mathbf{k}, \quad r = f(X), \ \theta = g(Y), \ z = Z, \ \mathbf{k} = \mathbf{e_3}; \\ &\qquad\qquad r_i \leqslant r \leqslant r_o, \ -\pi \leqslant \theta \leqslant \pi, \ -L \leqslant z \leqslant L \end{aligned} \tag{2}$$

characterizes the plane strain deformation of the continuum plate of thickness $2T$, width $2W$ and length $2L$ into a tube of inner radius r_i, outer radius r_o and length $2L$, as shown in Fig. 1.

The deformation gradient $\mathbf{F}$, defined by $\mathrm{d}\mathbf{r} = \mathbf{F}\mathrm{d}\mathbf{X}$, can be obtained from Eq. (2) as

$$\mathbf{F} = f'(X)\mathbf{e}_r \otimes \mathbf{e}_1 + f(X)g'(Y)\mathbf{e}_\theta \otimes \mathbf{e}_2 + \mathbf{k} \otimes \mathbf{e}_3, \tag{3}$$

where the prime denotes differentiation with respect to the argument of the function. To maintain the prescribed boundary correspondence, it is required that $f'(X) > 0$, $g'(Y) > 0$ and $r = f(X) > 0$. The left stretch tensor $\mathbf{V}$ can then be determined from the polar decomposition of $\mathbf{F}$ as

$$\mathbf{V} = f'(X)\mathbf{e}_r \otimes \mathbf{e}_r + f(X)g'(Y)\mathbf{e}_\theta \otimes \mathbf{e}_\theta + \mathbf{k} \otimes \mathbf{k}. \tag{4}$$

This leads to the following expression for the Hencky (true; logarithmic) strain $\mathbf{H} = \ln\mathbf{V}$:

$$\mathbf{H} = \ln f'(X)\mathbf{e}_r \otimes \mathbf{e}_r + \ln[f(X)g'(Y)]\mathbf{e}_\theta \otimes \mathbf{e}_\theta. \tag{5}$$

Assume that the deformation from the flat plate to the hollow cylinder is isochoric. Then, it follows that $J \equiv \det\mathbf{F} = 1$, which gives, with the use of Eq. (3),

$$f'(X)f(X)g'(Y) = 1. \tag{6}$$

Eq. (6) implies that

$$f'(X)f(X) = \frac{1}{g'(Y)} = C, \tag{7}$$

where C is a constant. This set of uncoupled ordinary differential equations, subject to the boundary conditions specified in Eq. (2), can be solved to yield

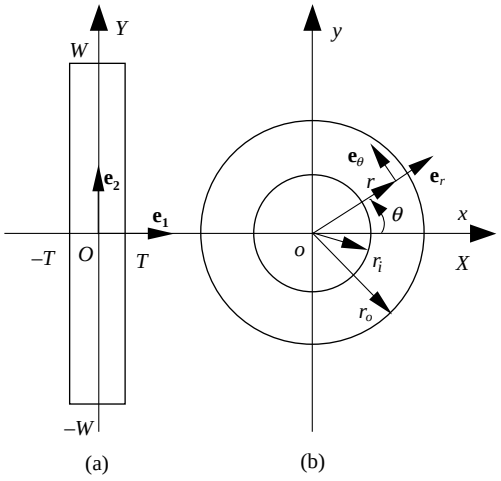

Fig. 1. Reference configuration (a) and deformed configuration (b).

$$r = f(X) = \sqrt{2\frac{W}{\pi}(X+T) + r_i^2}, \quad \theta = g(Y) = \frac{\pi}{W}Y, \tag{8}$$

where r_i is yet unknown and needs to be determined as part of the solution. The use of Eq. (8) in Eq. (5) then gives

$$\mathbf{H} = -\ln\left(\frac{\pi}{W}r\right)\mathbf{e}_r \otimes \mathbf{e}_r + \ln\left(\frac{\pi}{W}r\right)\mathbf{e}_\theta \otimes \mathbf{e}_\theta. \tag{9}$$

The Hencky strain $\mathbf{H}$ will be used to measure the large deformation, and the Cauchy (true) stress $\boldsymbol{\sigma}$, which is the same as the Kirchhoff stress conjugated to the Hencky strain when $J = 1$ (Gao, 1994), to describe the material response.

The stress–strain relation is taken to be linearly elastic, as was done in earlier studies on energetics of carbon nanotubes (e.g., Tersoff, 1992). This is based on the observation that the pure bending of the plate (representing the graphite sheet) into the cylinder (representing the SWCNT) involves large deformations but small strains. The latter are due to the small thickness of the cylinder (nanotube) and the existence of a neutral surface between the inner and outer surfaces of the cylinder. It then follows that the constitutive relation in terms of the Hencky strain $\mathbf{H}$ and the Cauchy stress $\boldsymbol{\sigma}$ can be written as (Gao, 1994)

$$\boldsymbol{\sigma} = \frac{2}{3}E\mathbf{H} - p\mathbf{I}, \tag{10}$$

where E is Young's modulus, p is the hydrostatic pressure, and $\mathbf{I}$ is the identity tensor defined by

$$\mathbf{I} = \mathbf{e}_r \otimes \mathbf{e}_r + \mathbf{e}_\theta \otimes \mathbf{e}_\theta + \mathbf{k} \otimes \mathbf{k}. \tag{11}$$

2.2. Boundary-value problem

The basic governing equations for the present problem, which embody the afore-mentioned kinematic and constitutive relations, include the equilibrium equations (with no body forces)

$$\operatorname{div}\boldsymbol{\sigma} = \mathbf{0}, \tag{12}$$

the kinematic equations

$$\mathbf{H} = \varepsilon_r \mathbf{e}_r \otimes \mathbf{e}_r + \varepsilon_\theta \mathbf{e}_\theta \otimes \mathbf{e}_\theta, \tag{13}$$

$$\varepsilon_r = -\ln\left(\frac{\pi}{W}r\right), \quad \varepsilon_\theta = \ln\left(\frac{\pi}{W}r\right), \tag{14a,b}$$

and the constitutive equations given in Eq. (10). The boundary conditions are

$$\mathbf{t}(-\mathbf{e}_r)|_{r=r_i} = \mathbf{0}, \quad \mathbf{t}(\mathbf{e}_r)|_{r=r_o} = \mathbf{0}, \tag{15a,b}$$

where $\mathbf{t}$, defined by $\mathbf{t}(\mathbf{m}) = \boldsymbol{\sigma}\mathbf{m}$, is the traction vector associated with the normal vector $\mathbf{m}$. The boundary-value problem defined by Eqs. (10) and (12)–(15a,b) can be analytically solved as follows.

Using Eqs. (10), (13) and (14a,b) in Eq. (12) results in

$$\frac{\mathrm{d}p}{\mathrm{d}r} = -\frac{2}{3}E\left[1 + 2\ln\left(\frac{\pi}{W}r\right)\right]\frac{1}{r}. \tag{16}$$

Integrating Eq. (16) from r_o to r yields

$$p(r) = p(r_o) - \frac{2}{3}E\left[1 + \ln\left(\frac{\pi^2}{W^2}rr_o\right)\right]\ln\frac{r}{r_o}. \tag{17}$$

The use of Eqs. (10), (13) and (14a,b) in Eq. (15b) leads to

$$p(r_o) = -\frac{2}{3}E\ln\left(\frac{\pi}{W}r_o\right). \tag{18}$$

Combining Eqs. (17) and (18) then gives

$$p(r) = -\frac{2}{3}E\left[\ln\left(\frac{\pi}{W}r\right) + \ln\left(\frac{\pi^2}{W^2}rr_o\right)\ln\frac{r}{r_o}\right] \tag{19}$$

as the expression of the hydrostatic pressure. Substituting Eqs. (11), (13), (14a,b) and (19) into Eq. (10) yields the stress components as

$$\begin{aligned}
\sigma_r &= \frac{2}{3}E\ln\left(\frac{\pi^2}{W^2}rr_o\right)\ln\frac{r}{r_o},\\
\sigma_\theta &= \frac{2}{3}E\left[2\ln\left(\frac{\pi}{W}r\right) + \ln\left(\frac{\pi^2}{W^2}rr_o\right)\ln\frac{r}{r_o}\right],\\
\sigma_z &= \frac{2}{3}E\left[\ln\left(\frac{\pi}{W}r\right) + \ln\left(\frac{\pi^2}{W^2}rr_o\right)\ln\frac{r}{r_o}\right],
\end{aligned} \tag{20a,b,c}$$

where r_o, together with r_i, is yet unknown and will be determined next from the remaining boundary conditions.

Using Eq. (20a) in Eq. (15a) results in

$$\frac{\pi^2}{W^2}r_i r_o = 1 \tag{21}$$

as the first relation required for solving r_i and r_o. The second needed relation is provided by the incompressibility (global) as

$$\frac{r_o^2 - r_i^2}{4T} = \frac{W}{\pi}. \tag{22}$$

Solving Eqs. (21) and (22) yields

$$r_i = \frac{W^2}{\pi^2}\frac{1}{r_o}, \quad r_o = \sqrt{\frac{W}{\pi}\left(2T + \sqrt{4T^2 + \frac{W^2}{\pi^2}}\right)}. \tag{23a,b}$$

Finally, the strain energy stored in the tube, Π_s, is given by

$$\Pi_s = \int_V \frac{1}{2}\sigma_{ij}\varepsilon_{ij}\,\mathrm{d}V = \int_V \frac{1}{2}(\sigma_r\varepsilon_r + \sigma_\theta\varepsilon_\theta)\,\mathrm{d}V, \tag{24}$$

where $\mathrm{d}V = (2L)(2\pi r)\,\mathrm{d}r$ is the volume element. Substituting Eqs. (14a,b) and (20a,b) into Eq. (24) results in

$$\frac{\Pi_s}{2L} = \frac{4\pi}{3}E\left[r_i^2\ln\left(\frac{\pi}{W}r_i\right) + \frac{1}{4}(r_o^2 - r_i^2)\right], \tag{25}$$

where use has also been made of Eq. (22).

2.3. Energy equivalence and Young's modulus

It has been found that the π-bond inversion of carbon atoms in a graphite sheet provides the resistance of the sheet to pure bending. Accordingly, by using the π-orbital axis vector technique the molecular potential

energy per carbon atom stored in a nanotube formed by pure bending of an undeformed (flat) graphite sheet, Π_ω, can be shown to be (see Odegard et al. (2002) and references cited therein)

$$\Pi_\omega = \frac{\overline{K^\omega}}{r_{nt}^2}, \tag{26}$$

where $\overline{K^\omega}$ is a force constant, and $r_{nt} = (r_i + r_o)/2$ is the mean radius of the nanotube. Some representative values of $\overline{K^\omega}$ obtained from published computational chemistry data are summarized in Odegard et al. (2002), which range from 0.011 to 0.022 eV · nm^2/atom, with an average of 0.018 eV · nm^2/atom. The total number of carbon atoms per nanotube is given by (Sawada and Hamada, 1992)

$$N = \frac{2\pi r_{nt}(2L)}{\Omega}, \tag{27}$$

where Ω is the occupied area per carbon atom in a nanotube, whose value is around 0.0262 nm^2/atom (Zhou et al., 2000; Zhang et al., 2002). Hence, it follows from Eqs. (26) and (27) that the total molecular potential energy of a nanotube (relative to the undeformed graphite sheet), Π_m, has the expression:

$$\frac{\Pi_m}{2L} = \frac{\Pi_\omega N}{2L} = \frac{2\pi\overline{K^\omega}}{\Omega r_{nt}}. \tag{28}$$

This amount of molecular potential energy available in the nanotube must be the same as the amount of strain energy stored in the continuum cylinder after rolling from the (stress-free) flat plate in order to have the required atomistic assembly (nanotube)—continuum (cylinder) equivalence. Hence, by equating Π_s in Eq. (25) and Π_m in Eq. (28), the elastic modulus, E, can be determined in terms of the known parameters as

$$E = \frac{3\overline{K^\omega}}{2\Omega r_{nt}}\left[r_i^2 \ln\left(\frac{\pi}{W} r_i\right) + \frac{1}{4}(r_o^2 - r_i^2)\right]^{-1}. \tag{29}$$

Since both the strain energy given in Eq. (25) and the molecular potential energy expressed in Eq. (28) are for the cylinder/nanotube, the resulting formula listed in Eq. (29) can be directly used to calculate the Young's modulus of the SWCNT, which is a rolled-up graphite sheet.

Note that Eqs. (23a,b) can be rewritten, in terms of r_{nt} and T, as

$$r_i = 2r_{nt} - r_o, \quad r_o = \frac{r_{nt}}{r_{nt}^2 + T^2}\left(r_{nt}^2 + T^2 + T\sqrt{r_{nt}^2 + T^2}\right). \tag{30a,b}$$

The substitution of Eqs. (30a,b) into Eq. (29) then gives the expression for the Young's modulus of the nanotube in terms of geometrical (r_{nt}, T) and molecular $(\overline{K^\omega}, \Omega)$ parameters, noting from Eq. (23a) that W is related to r_i and r_o (and thus r_{nt} and T). Clearly, for given $\overline{K^\omega}$ and Ω the values of E predicted by this model will depend on both r_{nt} and T. Sample numerical results for the Young's modulus predicted by the current model will be provided in the next section, where they will also be compared to the results obtained using Tibbetts' (1984) model which is based on the simple beam bending theory and is discussed further below.

Replacing a, R and L in Eq. (1) by $2T$, r_{nt} and $2L$, respectively, gives the strain energy Π in Tibbetts' model in terms of the current notation:

$$\frac{\Pi}{2L} = \frac{2\pi E T^3}{3r_{nt}}. \tag{31}$$

This is valid for the plane stress case (i.e., narrow beam bending), as noted earlier. For plane strain deformations, Eq. (31) needs to be modified by replacing E with $E/(1-\nu^2)$, which leads to

$$\frac{\Pi}{2L} = \frac{2\pi E T^3}{3(1-\nu^2) r_{nt}}, \tag{32}$$

where v is the Poisson's ratio of the graphite sheet. By equating Π in Eq. (32) and Π_m in Eq. (28), the Young's modulus predicted by Tibbetts' model for the plane strain case (i.e., wide beam or plate bending) is obtained as

$$E = \frac{3(1-v^2)\overline{K^\omega}}{T^3\Omega}. \tag{33}$$

This formula will be directly applied to generate numerical data in the next section. Clearly, Eq. (33) shows that Young's modulus E predicted by the Tibbetts model is independent of the nanotube mean radius r_{nt}, which differs from that predicted by the current model (see Eqs. (29) and (30a,b)). This difference will be further demonstrated using numerical data in the next section.

3. Numerical results

To illustrate the analytical formulas obtained in the preceding section, a parametric study of sample cases has been carried out. The relevant numerical results are presented below.

The variation of the Young's modulus with the nanotube radius, as predicted by the current model, is graphically shown in Fig. 2, where it is also compared to that determined using Tibbetts' (1984) model in the form given by Eq. (33) (with $v = 0.5$ used here). Following Yakobson et al. (1996), the effective thickness of the graphite sheet (i.e., $2T$; see Fig. 1) is taken to be 0.066 nm in the calculations leading to Fig. 2. Also, $\overline{K^\omega} = 0.018$ eV·nm^2/atom and $\Omega = 0.0262$ nm^2/atom, which are two typical values mentioned earlier, are used in obtaining the data shown in Figs. 2 and 3.

As illustrated in Fig. 2, the current model predicts $E = 5.5$ TPa, the value given in Yakobson et al. (1996) for carbon nanotubes having the effective thickness of 0.066 nm, when $r_{nt} = 0.0375$ nm. Furthermore, it is seen from Fig. 2 that the Young's modulus estimated by Tibbetts' model is a constant, independent of the nanotube radius. This is not the case with the current model. As shown in Fig. 2, with the increase of the radius the Young's modulus predicted by the current model decreases monotonically, which is in agreement with the trend revealed by the molecular dynamics studies reported in Cornwell and Wille (1997) and Yao and Lordi (1998). On the other hand, Fig. 2 also shows that for the effective thickness $2T = 0.066$ nm used here the current model and Tibbetts' model predict the same value of the Young's modulus when $r_{nt} = 0.0338$ nm, irrespective of the values of $\overline{K^\omega}$ and Ω. This, in fact, follows mathematically from equating Eqs. (29) and (33).

The influence of the nanotube wall thickness on the Young's modulus is illustrated in Fig. 3. From this figure it can be observed that the Young's modulus is reduced as the wall thickness increases. This predicted effect of the wall thickness, together with that of the nanotube radius, on the Young's modulus agrees with

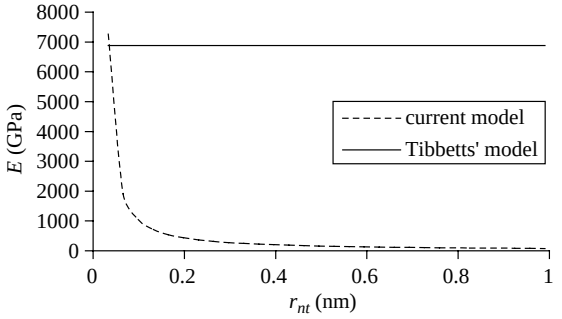

Fig. 2. Young's modulus vs. nanotube radius (with $2T = 0.066$ nm).

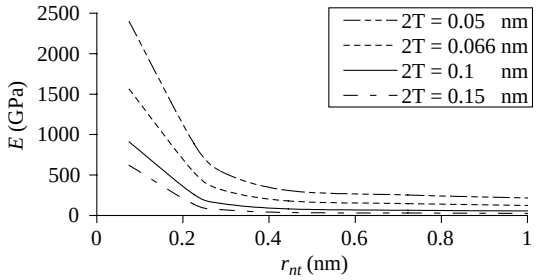

Fig. 3. Young's modulus varying with the nanotube wall thickness.

what was noted in Odegard et al. (2002), where it was stated, based on a different argument, that the Young's modulus should be inversely proportional to the cross-sectional area of the tube (and thus the product of the nanotube radius and wall thickness).

4. Summary

An analytical continuum model for computing strain energies and estimating Young's modulus of SWCNTs is developed using a multi-scale approach based on the energy equivalence. Finite deformation kinematics is invoked to describe the tube formation on the continuum level. A SWCNT is viewed as a continuum hollow cylinder formed by rolling up a flat graphite sheet (treated as an isotropic continuum plate). The Hencky (true) strain and the Cauchy (true) stress are employed to account for large deformations, while Hooke's law is applied to represent the constitutive behavior. Based on the equivalence of the strain energy and the molecular potential energy, an explicit formula for calculating the Young's modulus is derived, which, containing parameters at both continuum and molecular scales, directly links the macroscopic responses of nanotubes to their molecular structures.

To demonstrate the application of the new formula, a parametric study of sample cases is conducted. The trends of the Young's modulus changing respectively with the radius and thickness of a nanotube, as predicted by the current model, are in agreement with those predicted by several existing continuum mechanics and molecular dynamics models.

Acknowledgements

Part of this work was completed at AFRL/MLBC, Wright-Patterson AFB, OH in Summer 2002 when X.-L. Gao was an NRC/AFOSR Summer Faculty Fellow. He wishes to thank Dr. A.K. Roy, Dr. B. Maruyama and Branch Chief T. Benson Tolle of AFRL/MLBC for helpful discussions and hospitality. The helpful comments of one anonymous reviewer on an earlier version of this paper are also gratefully acknowledged.

References

Bernholc, J., Brenner, D., Nardelli, M.B., Meunier, V., Roland, C., 2002. Mechanical and electrical properties of nanotubes. Annu. Rev. Mater. Res. 32, 347–375.

Cornwell, C.F., Wille, L.T., 1997. Elastic properties of single-walled carbon nanotubes in compression. Solid State Commun. 101, 555–558.

Gao, X.-L., 1994. Finite deformation elasto-plastic solution for the pure bending problem of a wide plate of elastic linear-hardening material. Int. J. Solids Struct. 31, 1357–1376.

Gao, G., Cagin, T., Goddard, W.A., 1998. Energetics, structure, mechanical and vibrational properties of single-walled carbon nanotubes. Nanotechnology 9, 184–191.

Li, C., Chou, T.-W., 2003. A structural mechanics approach for the analysis of carbon nanotubes. Int. J. Solids Struct. 40, 2487–2499.

Maruyama, B., Alam, K., 2002. Carbon nanotubes and nanofibers in composite materials. SAMPE J. 38 (3), 59–68.

Odegard, G.M., Gates, T.S., Nicholson, L.M., Wise, K.E., 2002. Equivalent-continuum modeling of nano-structured materials. Compos. Sci. Tech. 62, 1869–1880.

Qian, D., Wagner, G.J., Liu, W.K., Yu, M.-F., Ruoff, R.S., 2002. Mechanics of carbon nanotubes. Appl. Mech. Rev. 55 (6), 495–533.

Robertson, D.H., Brenner, D.W., Mintmire, J.W., 1992. Energetics of nanoscale graphitic tubules. Phys. Rev. B 45, 12592–12595.

Sawada, S., Hamada, N., 1992. Energetics of carbon nano-tubes. Solid State Commun. 83, 917–919.

Tersoff, J., 1992. Energies of fullerenes. Phys. Rev. B 46, 15546–15549.

Thostenson, E.T., Ren, Z., Chou, T.-W., 2001. Advances in the science and technology of carbon nanotubes and their composites: a review. Compos. Sci. Tech. 61, 1899–1912.

Tibbetts, G.G., 1984. Why are carbon filaments tubular? J. Cryst. Growth 66, 632–638.

Vaia, R.A., Tolle, T.B., Schmitt, G.F., Imeson, D., Jones, R.J., 2001. Nanoscience and nanotechnology: materials revolution for the 21st century. SAMPE J. 37 (6), 24–31.

Yakobson, B.I., Brabec, C.J., Bernholc, J., 1996. Nanomechanics of carbon tubes: instabilities beyond linear response. Phys. Rev. Lett. 76, 2511–2514.

Yao, N., Lordi, L., 1998. Young's modulus of single-walled carbon nanotubes. J. Appl. Phys. 84, 1939–1943.

Zhang, P., Huang, Y., Geubelle, P.H., Klein, P.A., Hwang, K.C., 2002. The elastic modulus of single-wall carbon nanotubes: a continuum analysis incorporating interatomic potentials. Int. J. Solids Struct. 39, 3893–3906.

Zhou, X., Zhou, J., Ou-Yang, Z.-C., 2000. Strain energy and Young's modulus of single-wall carbon nanotubes calculated from electronic energy-band theory. Phys. Rev. B 62, 13692–13696.